Theoretical modeling of two-color coherent anti-Stokes Raman spectroscopy spectra measured with a frequency-doubled, multimode pump laser

G. S. Agarwal

Department of Mathematics, University of Manchester Institute of Science and Technology, Manchester, UK

R. L. Farrow

Combustion Research Facility, Sandia National Laboratories, Livermore, California 94550

Received June 9, 1986; accepted August 5, 1986

We have theoretically modeled coherent anti-Stokes Raman spectroscopy spectra of nitrogen measured with a frequency-doubled Nd:YAG pump laser. The fluctuations of the multimode pump field are modeled using a field variable having non-Gaussian statistics derived from a functional dependence on a Gaussian field. Both isolated and multiple, overlapping transitions are treated. The model qualitatively predicts the non-Gaussian effects observed in experiments but somewhat overemphasizes the magnitude of these features.

Coherent anti-Stokes Raman spectroscopy (CARS) is finding increasing application as a tool for quantitative measurements of temperature and species concentrations in gases.[1,2] Extracting these observables from experimental CARS spectra requires accurate models for calculating theoretical third-order susceptibilities and consideration of the spectral and temporal properties of the laser sources for calculating spectra. These effects are well understood in CARS spectra for laser fields obeying Gaussian statistics.[2-6] To our knowledge, however, no complete theoretical treatments for non-Gaussian fields have been reported. The statistics of incident radiation fields have been shown to influence the characteristics of detected light in such nonlinear processes as stimulated Raman scattering,[7] diffraction from a laser-induced grating,[8] and two-photon absorption.[9] Thus non-Gaussian-field statistics should be an important consideration in the quantitative interpretation of CARS spectra.

Experiments have shown that the statistics of the fluctuations of a multimode laser field can affect intensities and line shapes in molecular CARS spectra.[10,11] In these measurements, two pump beams from a frequency-doubled, multimode Nd:YAG laser were used with a variable relative delay in a crossed-beam CARS geometry. Spectra measured with different delays (small compared with the temporal pulse widths) gave information on the effects of correlation between the beams and clearly established the presence of non-Gaussian statistics in the pump field. Because of the lack of a model for describing the higher-order correlation functions of the particular pump field, these results were not compared with a non-Gaussian theory. Subsequently, the effects of using frequency-doubled radiation as the CARS pump fields were investigated for the particular case of nonresonant CARS intensities.[12]

In this paper we report the application of a simple model for the frequency-doubled pump field for calculating both resonant and nonresonant CARS spectra. The pump field is expressed classically as a function of a Gaussian field. The resulting field exhibits significant non-Gaussian characteristics but has analytic high-order correlation functions that permit spectra to be calculated easily. This is a reasonable approach for the experiments of Refs. 10 and 11 and others for which the pump field is produced by frequency doubling a source with nearly Gaussian statistics (i.e., the fundamental output of a Nd:YAG laser operating in many independent modes[13]). We calculate spectra using both Gaussian and non-Gaussian statistics for the pump fields and show that the latter provide a reasonably good description of the results of Rahn *et al.*[10] We also present results for the case of multiple, overlapping transitions.

For an isolated Raman transition, the anti-Stokes field amplitude E_{aS} can be written as[3]

$$E_{aS}(t) = \chi_{nr}E_1^2(t)E_2^*(t) + \frac{i\chi_r}{T_2} \times \int_0^t d\tau E_1(t)E_1(t-\tau)E_2^*(t-\tau) \times \exp[-(1/T_2 + i\Delta)\tau], \quad (1)$$

where $\Delta = \omega_R - (\omega_1 - \omega_2)$, χ_{nr} is proportional to the nonresonant part of the third-order susceptibility responsible for four-wave mixing, $1/T_2$ is the half-width of the Raman line, and ω_1, ω_2, E_1, and E_2 are, respectively, the frequencies and amplitudes of the pump and Stokes fields. The parameter χ_r determines the strength of the resonant contribution to E_{aS}, and we assume that saturation effects on χ_r are negligible. We model the fundamental field produced by a Nd:YAG laser as a field $V(t)$ with Gaussian statistics and its amplitude (after frequency doubling) as $V^2(t)$. Thus the pump amplitude can be written as

$$E_D(t) = \beta V^2(t), \quad (2)$$

0740-3224/86/111596-06$02.00

where β is a measure of the efficiency of the second-harmonic generation. This model corresponds to the case of phase-matched, coherent frequency doubling in the limit of negligible depletion of the fundamental field.[14] Using Eq. (2) and the moment theorem for Gaussian random processes,[15] the multitime correlation functions of $E_D(t)$ can be calculated. We quote the result for the fourth-order correlation function of the field $E_D(t)$, which is an eighth-order correlation function of $V(t)$:

$$\begin{aligned}\langle E_D^*(t)E_D^*(t+t_1)E_D(t+t_2)E_D(t+t_3)\rangle \\ = I_1^2[\gamma_1^2(t_1-t_2)\gamma_1^2(-t_3)+\gamma_1^2(-t_2)\gamma_1^2(t_1-t_3) \\ +4\gamma_1(t_1-t_2)\gamma_1(t_1-t_3)\gamma_1(-t_2)\gamma_1(-t_3)]. \quad (3)\end{aligned}$$

Here I_1 is the average intensity of the field E_D:

$$I_1 = \langle E_D^*(t)E_D(t)\rangle = 2\beta^2\langle V^*(t)V(t)\rangle^2, \quad (4)$$

and $\gamma_1(t_1-t_2)$ is the normalized correlation function of the Gaussian field V:

$$\gamma_1(t_1-t_2) = \frac{\langle V^*(t_1)V(t_2)\rangle}{\langle|V(t)|^2\rangle}. \quad (5)$$

The angle brackets denote time averaging over periods long compared with T_2 and with the time scales for all field fluctuations. The total pump field in Eq. (1) is equal to

$$E_1(t) = E_D(t) + E_D(t-\delta), \quad (6)$$

where δ is the temporal delay between the two pump beams. In the product $E_1(t)E_1(t-\tau)$ found in Eq. (1), only the contribution $E_D(t)E_D(t-\tau-\delta)+E_D(t-\tau)E_D(t-\delta)$ will be detected, because of the crossed-beam phase matching.

The CARS signal can be calculated by using Eqs. (1), (3), and (6). Our calculations show that

$$\begin{aligned}I_{aS}(\delta) &= \lim_{t\to\infty}\langle E_{aS}^*(t)E_{aS}(t)\rangle \\ &= 4I_1^2I_2\Bigg(\chi_{nr}^2[1+\gamma_1^2(\delta)\gamma_1^2(-\delta)+4\gamma_1(\delta)\gamma_1(-\delta)] \\ &+\frac{i\chi_r}{2T_2}\chi_{nr}\int_0^\infty d\tau\exp[-(1/T_2+i\Delta)\tau]\gamma_2(-\tau) \\ &\times[\gamma_1^2(\tau)+\gamma_1^2(\tau+\delta)\gamma_1^2(-\delta)+4\gamma_1(\tau)\gamma_1(\tau+\delta)\gamma_1(-\delta) \\ &+(\delta\to-\delta)]+\text{c.c.}+\frac{\chi_r^2}{4T_2^2}\Bigg\{\int_0^\infty d\eta\exp[-(1/T_2+i\Delta)\eta] \\ &\times\int_0^\eta d\tau\exp[-(1/T_2-i\Delta)\tau]\gamma_2(\tau-\eta)[\gamma_1^2(\eta-\tau) \\ &+\gamma_1^2(\delta+\eta)\gamma_1^2(-\tau-\delta)+4\gamma_1(\eta-\tau)\gamma_1(\eta+\delta)\gamma_1(-\tau-\delta) \\ &+\gamma_1^2(-\delta)\gamma_1^2(\eta+\delta-\tau)+\gamma_1^2(-\tau)\gamma_1^2(\eta) \\ &+4\gamma_1(\eta+\delta-\tau)\gamma_1(-\tau)\gamma_1(\eta)\gamma_1(-\delta) \\ &+(\delta\to-\delta)]+\text{c.c.}\Bigg\}\Bigg), \quad (7)\end{aligned}$$

where $\gamma_2(\tau)$ is the normalized correlation function for the Stokes field E_2:

$$\gamma_2(\tau) = \frac{\langle E_2^*(t+\tau)E_2(t)\rangle}{\langle E_2^*(t)E_2(t)\rangle}. \quad (8)$$

The notation $(\delta\to-\delta)$ implies that the preceding terms within the same brackets are to be repeated with δ replaced by $-\delta$.

We first note that for long delays $\delta\to\infty$, $\gamma(\delta)\to 0$, and result (7) simplifies to

$$\begin{aligned}I_{aS}(\infty) &= 4I_1^2I_2\Bigg(\chi_{nr}^2+\frac{i\chi_r}{T_2}\chi_{nr} \\ &\times\int_0^\infty d\tau\exp[-(1/T_2+i\Delta)\tau]\gamma_2(-\tau)\gamma_1^2(\tau)+\text{c.c.} \\ &+\frac{\chi_r^2}{2T_2^2}\Bigg\{\int_0^\infty d\eta\exp[-(1/T_2+i\Delta)\eta] \\ &\times\int_0^\eta d\tau\exp[-(1/T_2-i\Delta)\tau]\gamma_2(\tau-\eta)[\gamma_1^2(\eta-\tau) \\ &+\gamma_1^2(-\tau)\gamma_1^2(\eta)]+\text{c.c.}\Bigg\}\Bigg). \quad (9)\end{aligned}$$

This limit also corresponds to the case when the pump beams are supplied by independent laser sources. For purposes of comparison, we also present the expression for $I_{aS}(\delta)$ for a Gaussian pump field, i.e., where we put $E_1(t) = V(t)$:

$$\begin{aligned}I_{aS}^G(\delta) &= 4I_1^2I_2\Bigg(\chi_{nr}^2[1+\gamma_1(\delta)\gamma_1(-\delta)] \\ &+\frac{i\chi_r}{2T_2}\chi_{nr}\int_0^\infty d\tau\exp[-(1/T_2+i\Delta)\tau]\gamma_2(-\tau) \\ &\times[\gamma_1(\tau)+\gamma_1(\tau+\delta)\gamma_1(-\delta)+(\delta\to-\delta)]+\text{c.c.} \\ &+\frac{\chi_r^2}{4T_2^2}\Bigg\{\int_0^\infty d\eta\exp[-(1/T_2+i\Delta)\eta] \\ &\times\int_0^\eta d\tau\exp[-(1/T_2-i\Delta)\tau]\gamma_2(\tau-\eta)[\gamma_1(\eta-\tau) \\ &+\gamma_1(\delta+\eta)\gamma_1(-\tau-\delta)+\gamma_1(-\delta)\gamma_1(\delta-\tau+\eta) \\ &+\gamma_1(\eta)\gamma_1(-\tau)+(\delta\to-\delta)]+\text{c.c.}\Bigg\}\Bigg). \quad (10)\end{aligned}$$

Using Eqs. (9) and (10), we obtain the following interesting relation between the two models:

$$\lim_{\delta\to\infty} I_{aS}(\delta) = \lim_{\delta\to\infty} I_{aS}^G(\delta) \quad (11)$$

if $\gamma_1^2(\tau)$ in the non-Gaussian model is replaced by $\gamma_1(\tau)$. This result shows that the two models give identical results in the limit of large delay if the corresponding spectral profiles for $E_1(t)$ are identical. In practice, large delay corresponds to $\delta\gg\max(T_2,\tau_c)$, where τ_c is a coherence time for laser-field fluctuations. In addition,

$$I_{aS}^G(0) = 2\lim_{\delta\to\infty} I_{aS}^G(\delta), \quad (12)$$

and hence

$$\lim_{\delta\to\infty} I_{aS}(\delta) = \tfrac{1}{2}I_{aS}^G(0). \quad (13)$$

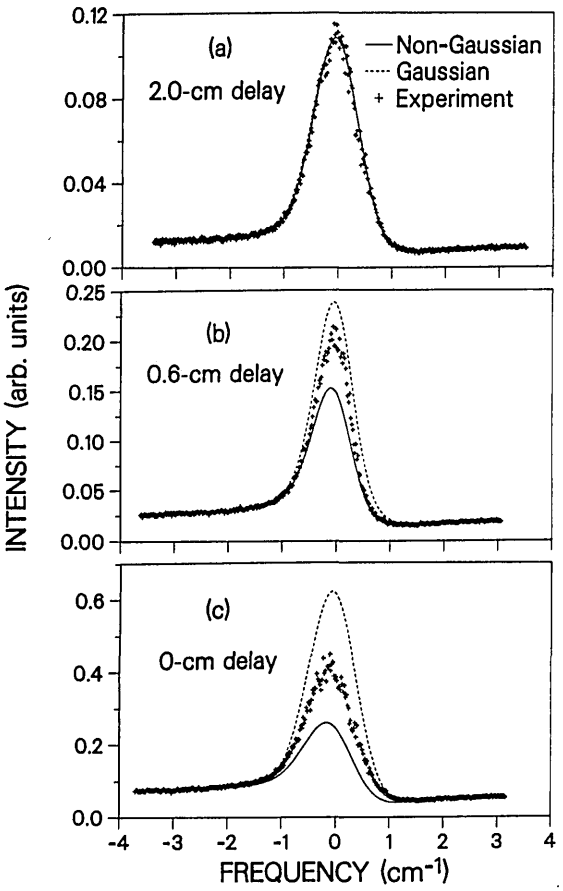

Fig. 1. Comparison of experimental CARS spectra with theoretical spectra using Gaussian and non-Gaussian stochastic processes to model the pump field. Note that the experimental peak-to-background intensity ratio decreases as the pump-beam delay is decreased. Although the Gaussian theoretical spectra show little variation with delay, the non-Gaussian spectra follow the behavior of the data. The measurements were performed on the $O(18)$ transition of nitrogen at 300 Torr and 296 K. At this pressure, T_2 for molecular relaxation (~400 psec) is much longer than the time scale for pump-laser fluctuations (10–20 psec).

Thus, to within a numerical factor, the non-Gaussian model with sufficiently delayed pump beams gives spectra identical to those of the Gaussian model. This is an important result, implying that non-Gaussian effects may be suppressed in dual-pump-beam CARS geometries. This result is consistent with the experimental findings of Ref. 11 and was also obtained theoretically by Yuratich.[3]

Equations (7) and (10) reduce to analytic expressions when the laser spectral profiles are assumed to be Lorentzian. However, pulsed Nd:YAG and dye lasers are generally better moldeled with Gaussian profiles, which require numerical evaluation of the integrals in Eqs. (7) and (10). We assumed spectral profiles of the form $\gamma_i(\tau) = \exp(-\tau^2\Gamma_i^2)$, $i = 1, 2$ for the laser fields. The linewidth parameter Γ_1 for the non-Gaussian pump field was taken to be $1/\sqrt{2}$ times that for the Gaussian field. This factor facilitated comparisons between the models by making the spectral bandwidth of the non-Gaussian pump field $[E_1(t) = E_D(t)]$ equal to that of the Gaussian pump field $[E_1(t) = V(t)]$.

Calculations based on Eqs. (7) and (10) were performed on a VAX 11/780 computer using standard integration and high-speed error-function routines. Figure 1 compares the behavior of $I_{aS}(\delta)$ and $I_{aS}{}^G(\delta)$ with the experimental results of Rahn *et al.*[10] for different values of δ. The measurements were performed with a scanning CARS system using a doubled Nd:YAG laser with a FWHM linewidth of 1.0 cm^{-1}. The spectrum of an isolated nitrogen $O(18)$ transition along with the nonresonant background intensity was measured at 300 Torr. Assuming a collisional-broadening coefficient[16] of 0.06 cm^{-1}/atm (HWHM), the time for molecular relaxation at this pressure is given by $T_2 = 400$ psec. In contrast, the time scale for pump-laser fluctuations (τ_c) is much shorter, of the order of 12 psec.

The crosses in Fig. 1 indicate CARS spectra measured with three different delays. For purposes of comparison, the data and theoretical curves are normalized by the nonresonant background intensity for all three delay values. Also, the amplitudes of the theoretical resonant susceptibilities are adjusted once for best agreement with the data in Fig. 1(a) but are not changed otherwise. As the delay approaches zero [Figs. 1(b) and 1(c)], the peak-to-background ratio for the data and for the non-Gaussian model (solid lines) decreases. However, the non-Gaussian model predicts too much reduction, by about a factor of 2 in comparison with the data. Note that the Gaussian model (dashed lines) changes relatively little and thus overestimates the peak-to-background ratio as the delay is reduced.

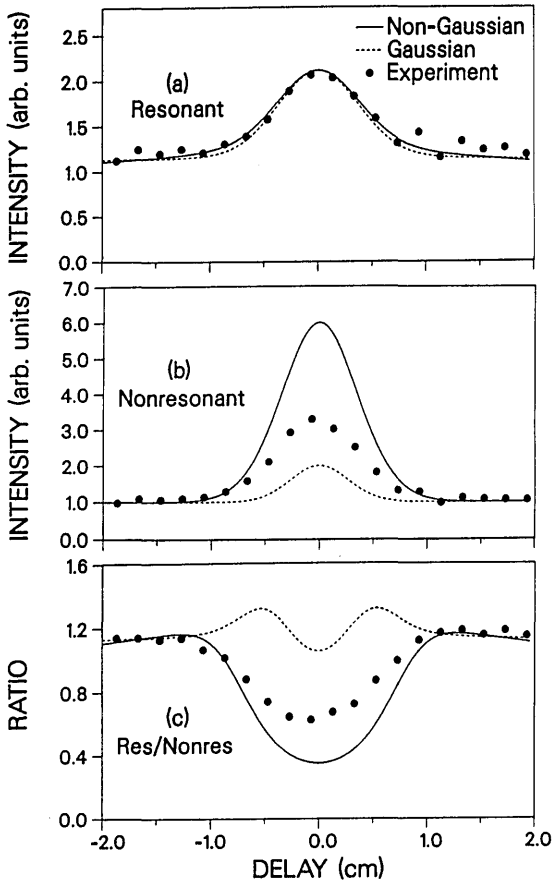

Fig. 2. Comparison of measured resonant and nonresonant intensities and ratios with theoretical results using Gaussian and non-Gaussian stochastic processes to model the pump field. The measurements were performed on the $O(18)$ transition of nitrogen at 500 Torr and 296 K. While the non-Gaussian theory overpredicts the enhancement of resonant intensity at zero delay, it describes the intensity ratio more successfully than the Gaussian theory.

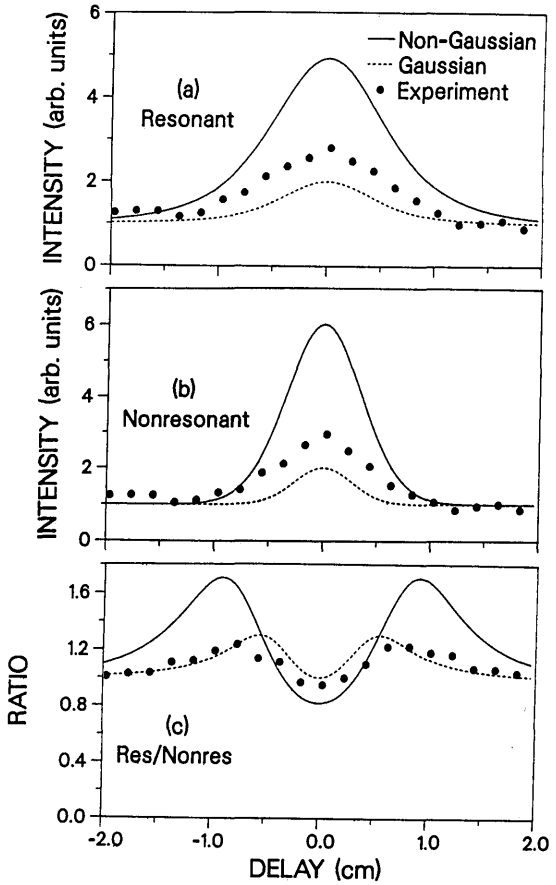

Fig. 3. Comparison of measured resonant and nonresonant intensities and ratios with theoretical results using Gaussian and non-Gaussian stochastic processes to model the pump field. The measurements were performed on the $O(18)$ transition of nitrogen at 4560 Torr and 296 K. Here, $T_2 = 30$ psec, comparable with the time scale of pump-laser fluctuations.

This behavior can be better understood by separately examining the dependences of the resonant and nonresonant intensities versus delay. Experimentally, this comparison was accomplished[10] by splitting the anti-Stokes beam and using dual polarizers and detectors to measure the resonant and nonresonant intensity components separately. Figure 2 shows the experimental intensities and those calculated from Eqs. (7) and (10) by alternately setting χ_{nr} and χ_r to zero. The circles in Fig. 2(a) are the measured resonant intensities plotted versus delay. The theroetical non-Gaussian (solid lines) and Gaussian (dashed lines) intensities are plotted with vertical scale factors varied for best fit. Note that the resonant intensity profiles predicted by the two models agree closely with each other and with the data. This result supports the hypothesis of Ref. 10 that the behavior of the resonant intensities with $T_2 \gg \tau_c$ is insensitive to the detailed nature of fluctuation statistics.

Nonresonant intensities are compared in Fig. 2(b), where the plots were normalized for best agreement with the intensity at large delay. In this case, the two models diverge widely from each other and from the experiment. The intensity of the non-Gaussian model is enhanced by a factor of 6 at zero delay relative to large delay (in this case, $\delta \gg 1/\Gamma_1$), whereas the Gaussian model is enhanced by a factor of 2. The observed enhancement of 3.4 falls between these results. However, the width of the experimental profile agrees more closely with the non-Gaussian model than with the Gaussian model. Plotting the ratio of resonant to nonresonant intensity for all three cases gives the curves shown in Fig. 2(c). The primary difference between the two models arises from differences in the predicted nonresonant intensity profiles. The larger width and enhancement factor for the non-Gaussian profile results in a deeper, broader dip in the ratio scan, in better agreement with observations.

Measurements at 4560 Torr are shown by the data points in Fig. 3. We find that the observed resonant intensity at zero delay exhibits greater enhancement than seen previously and greater than predicted by Gaussian theory. However, the non-Gaussian model overpredicts the degree of enhancement. The result is that the plot of ratio versus delay more closely resembles that of the Gaussian model, in contrast to previous results. An additional result is that the dip in the ratio curve is less pronounced than at low pressure. Calculations at even higher pressures showed the ratio curve flattening even more, as the resonant and nonresonant intensities began to behave similarly with respect to delay. This trend occurs as the Raman linewidth ($1/T_2$, assumed proportional to pressure) exceeds the pump-laser linewidth. In the limit $1/T_2 \gg \Gamma_1$ we find that the ratio of resonant to nonresonant intensities is independent of delay. In this case, CARS spectral profiles are also independent of delay and are therefore unaffected by non-Gaussian pump-field statistics.

The results of Figs. 1–3 can be understood in physical terms as a tendency of the Gaussian theory to ignore, and the non-Gaussian model to overemphasize, certain intensity enhancements with coherent pump beams. This anomalously enhanced signal generation occurs under conditions of rapid polarizability response to non-Gaussian pump-field fluctuations. The amplitude of polarizability oscillations induced through the nonresonant susceptibility, or resonant susceptibility with $T_2 \leq \tau_c$, can rapidly respond to intense spikes in the driving force produced by one pump beam. (We assume a narrow-band Stokes laser.)

When matched by in-phase fluctuations from the other pump beam, these spikes result in unexpectedly high anti-Stokes intensities compared with Gaussian-field predictions [Figs. 2(b), 3(a), and 3(b)]. However, for resonant intensities with $T_2 \gg \tau_c$, the molecule cannot respond to these rapid fluctuations, and the resulting anti-Stokes intensities are similar for Gaussian and non-Gaussian fields [Fig. 2(a)].

The overly large intensity enhancements predicted by the non-Gaussian theory probably result from the simple treatment of the frequency-doubled field by our model [Eq. (2)]. The actual pump field is probably smoother than predicted by this expression, owing to depletion effects in the fundamental field $V(t)$ and phase walk-off effects associated with type II doubling.[14] It has also been suggested[12] that saturation in the Nd:YAG amplifier would tend to reduce field excursions before frequency doubling. These processes could result in a field with non-Gaussian fluctuations intermediate to the models considered here and thus would produce more-moderate intensity enhancements. The realistic inclusion of these effects, however, was found to be beyond the scope of this work. We note that Hall[12] obtained expressions for the enhancement of purely nonresonant intensities that decreased with increasing conversion efficiency of the frequency-doubling process. This result was attributed to

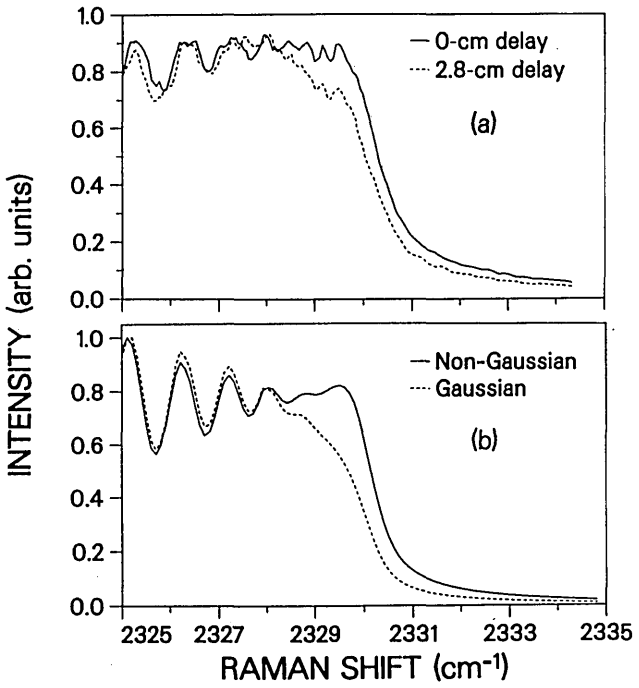

Fig. 4. Comparison of experimental spectra of the nitrogen Q-branch bandhead with theoretical spectra using Gaussian and non-Gaussian stochastic processes to model the pump field. The data were measured in the postflame gases of a premixed methane–air flame having a gas temperature of 1730 K (determined by CARS thermometry). For the calculations, we assumed that molecular relaxation was the same for all transitions, $T_2 = 330$ psec.

fundamental field depletion effects in the second-harmonic field.

In the analysis thus far, we have assumed only a single resonant Raman transition. For many overlapping transitions with complex frequencies $\omega_{R,n} - i/T_{2,n}$ and detunings $\Delta_n = \omega_{R,n} - (\omega_1 - \omega_2)$ we find that the CARS signal can be obtained from Eq. (7) by using the replacement

$$\frac{\chi_r}{T_2}\exp[-(1/T_2 + i\Delta)\tau] \rightarrow \sum_n \frac{\chi_{r,n}}{T_{2,n}}\exp[-(1/T_{2,n} + i\Delta_n)\tau] \tag{14}$$

in the term involving χ_r and

$$\frac{\chi_r^2}{T_2^2}\exp[-(1/T_2 + i\Delta)]\eta\exp[-(1/T_2 + i\Delta)\tau] \rightarrow \sum_n\sum_{n'} \frac{\chi_{r,n}\chi_{r,n'}}{T_{2,n}T_{2,n'}}\exp[-(1/T_{2,n} + i\Delta_n)\eta] \times \exp[-(1/T_{2,n'} + i\Delta_{n'})\tau], \tag{15}$$

where n is interchanged with n' before taking the complex conjugate, in the term involving χ_r^2. Expression (15) and Eq. (7) permit the study of the effects of non-Gaussian statistics on multiple, overlapping transitions. This treatment assumes, however, that the line spacings are larger than $1/T_{2,n}$, so that amplitude interference (i.e., collisional-narrowing) effects[16] are negligible. Thus the term overlapping applies more properly to the transitions after inclusion of the pump-laser line shape.

In measurements of overlapping transitions in the $v = 0 \rightarrow$ Q-branch band of nitrogen, we observed differences in spectra measured with and without pump-beam delay. When the spectra are compared by normalizing to maximum intensities [Fig. 4(a)], the intensity of the bandhead region of the 0-cm delay spectrum is enhanced relative to the 2.8-cm delay spectrum. As will be shown below, the enhanced intensity takes the appearance of a bandhead peak that is in disagreement with calculated spectra based on Gaussian statistics. A possibly related observation was reported by Stufflebeam *et al.*,[17] who described an anomalous peak at the bandhead of carbon monoxide at elevated temperatures. This peak was not predicted by any of several Gaussian spectral models investigated. (It should be mentioned, however, that this effect could alternatively have arisen from not including the correct pump-laser line-shape convolution.[5])

We performed a comparison of our theroetical results for multiple transitions with the data of Fig. 4(a). The data were measured in a flame at 1730 K and atmospheric pressure, so that collisional-narrowing effects were unimportant. At this temperature, the ground-state band contains contributions from 50–60 transitions. Owing to the excessive computational time required for including large numbers of transitions in expression (15) and Eq. (7), we included only the first 18 of these transitions. This approximation is not unreasonable because we are interested in a limited spectral region, and the included transitions adequately describe the bandhead profile. To reduce computation time further, the data measured with nonzero delay were compared with the results of Gaussian theory [expression (15) and Eq. (10)] with zero delay. This approach is based on the result of Eq. (13), where the large-delay limit of the non-Gaussian spectrum is equal within a scaling factor to the zero-delay Gaussian spectrum. The actual delay used in the measurement was greater than the coherence length of the pump laser (~1.6 cm) and thus approximated the limit of large delay. Parameters employed for the computations included Raman linewidths based on measurements by Owyoung and Rahn,[18] calculated transition amplitudes as described by Hall,[19] and Gaussian pump- and probe-laser line shapes with full bandwidths of 0.6 and 0.07 cm^{-1}, respectively, corresponding to experimental values.

The calculated bandhead spectra are shown in Fig. 4(b). The spectrum using a non-Gaussian field exhibits enhanced intensity for Raman shifts above 2328 cm^{-1}, in much the same way as the 0-cm delay experimental spectrum. While it is qualitatively similar, the theoretical enhancement is somewhat larger than what is actually observed. This small exaggeration is probably related to the previously observed overprediction of non-Gaussian effects by the model. Nevertheless, the results convincingly demonstrate the capability of non-Gaussian fluctuations to produce such bandhead peaks and are in good agreement with the present observations.

In conclusion, we have demonstrated a simple model for studying the effects of non-Gaussian pump-field statistics on CARS spectra. The model qualitatively reproduces the characteristics of these effects as experimentally studied with variable pump-beam delays. The model also successfully describes the anomalous enhancement of nonresonant and highly damped resonant intensities at zero delay, the increased width of these scans versus delay, and an extra

peak appearing at the Q-branch bandhead of nitrogen. In addition, we demonstrated that non-Gaussian effects can be eliminated in a dual-pump-beam experiment by using a temporal delay between the beams such that $\delta \gg \max(T_2, \tau_c)$.

Recent measurements in other laboratories[20] of nonresonant intensities versus delay indicate that certain Nd:YAG lasers do not exhibit significant non-Gaussian behavior, i.e., they have maximum enhancement factors of 2. Indeed, different lasers of the same model in our laboratories produce different maximum enhancements. It follows that non-Gaussian effects may be absent in many instances, and standard Gaussian theory will be valid. The latter condition is also expected to apply when Raman widths are large compared with the pump-laser linewidth, as in high-pressure measurements or when a sufficiently narrow-band pump laser is used.

Nevertheless, non-Gaussian statistical models such as those described in this work will be required for analysis of CARS spectra in some circumstances. Examples include an experiment using a non-Gaussian pump laser and collinear phase matching (employing a single pump beam) or a crossed-pump-beam experiment in which the required relative beam delay would be large compared with the laser-pulse durations. For quantitative applications, it is essential that the anomalous enhancements predicted by theory be in close agreement with those actually observed (e.g., in a comparison of spectra with and without delayed pump beams). To this end, we are currently investigating models that more realistically treat the second-harmonic fields from multimode Nd:YAG lasers. Since such *ab initio* theories are likely to be too complex for practical use, we are also examining the utility of empirical correlation functions. One such function under consideration is obtained by varying the contribution of non-Gaussian terms in Eq. (7) by an experimentally determined coefficient. The lengthy time of computations is another problem, although this can be addressed by using more-efficient algorithms or by relying on precalculated libraries of spectra. Alternatively, the need for non-Gaussian analysis could be obviated in the experiments through the use of transform-limited lasers with smooth temporal envelopes.

ACKNOWLEDGMENTS

R. L. Farrow acknowledges helpful discussions with R. P. Trebino of Sandia National Laboratories. His research is supported by the U.S. Department of Energy, Office of Basic Energy Sciences, Chemical Sciences Division. The research of G. S. Agarwal is partially supported by the Science and Engineering Research Council (UK).

G. S. Agarwal is also with the School of Physics, University of Hyderabad, Hyderabad-500134, India.

REFERENCES

1. See, for example, S. A. J. Druet and J.-P. E. Taran, "CARS spectroscopy," Prog. Quantum Electron. **7,** 1–72 (1981).
2. R. J. Hall and A. C. Eckbreth, "CARS: application to combustion diagnostics," in *Laser Applications*, J. F. Ready and R. K. Erf, eds. (Academic, New York, 1984), Vol. 5, pp. 213–309.
3. M. A. Yuratich, "Effects of laser linewidth on CARS," Mol. Phys. **38,** 625–655 (1979).
4. H. Kataoka, S. Maeda, and C. Hirose, "Effects of laser linewidth on the CARS spectral profile," Appl. Spectrosc. **36,** 565–569 (1982).
5. R. E. Teets, "Accurate convolutions of CARS spectra," Opt. Lett. **9,** 226–228 (1984).
6. G. S. Agarwal and S. Singh, "Effects of pump fluctuations on line shapes in CARS," Phys. Rev. A **25,** 3195–3205 (1982).
7. M. G. Raymer and L. A. Westling, "Quantum theory of Stokes generation with a multimode laser," J. Opt. Soc. Am. B **2,** 1417–1421 (1985).
8. R. Trebino, E. K. Gustafson, and A. E. Siegman, "Fourth-order partial-coherence effects in the formation of integrated-intensity gratings with pulsed light sources," J. Opt. Soc. Am. B **3,** 1295–1304 (1986).
9. D. S. Elliott, M. W. Hamilton, K. Arnett, and S. J. Smith, "Correlation effects of a phase-diffusing field on two-photon absorption," Phys. Rev. A **32,** 887–895 (1985).
10. L. A. Rahn, R. L. Farrow, and R. P. Lucht, "Effects of laser field statistics on CARS intensities," Opt. Lett. **9,** 223–225 (1984).
11. R. L. Farrow and L. A. Rahn, "Interpreting CARS spectra measured with multimode Nd:YAG pump lasers," J. Opt. Soc. Am. B **2,** 903–907 (1985).
12. R. J. Hall, "The statistical behaviour of nonresonant CARS intensities," Opt. Commun. **56,** 127–130 (1985).
13. A. A. Grütter, H. P. Weber, and R. Dändliker, "Imperfectly mode-locked laser emission and its effects on nonlinear optics," Phys. Rev. **185,** 629–643 (1969).
14. S. A. Akhmanov, A. I. Kovrygin, and A. P. Suhkorukov, "Optical harmonic generation and optical frequency multipliers," in *Quantum Electronics: A Treatise*, H. Rabin and C. L. Tang, eds. (Academic, New York, 1975), pp. 476–586.
15. N. G. Van Kampen, *Stochastic Processes in Physics and Chemistry* (North-Holland, New York, 1981).
16. G. J. Rosasco, W. Lempert, and W. S. Hurst, "Line interference effects in the vibrational Q-branch spectra of N_2 and CO," Chem. Phys. Lett. **97,** 435–440 (1983).
17. J. H. Stufflebeam, R. J. Hall, and A. C. Eckbreth, "Investigation of the CARS spectrum of carbon monoxide at high pressure and temperature," U.S. Air Force Tech. Rep. AFRPL TR-84-042 (July 1984).
18. A. Owyoung and L. A. Rahn, "High-resolution inverse Raman spectroscopy in a methane–air flame," IEEE J. Quantum Electron. **QE-15,** 28d (1979).
19. R. J. Hall, "CARS spectra of combustion gases," Combust. Flame **35,** 47–60 (1979).
20. D. A. Greenhalgh, Atomic Energy Research Establishment Harwell, Oxfordshire, UK (personal communication).